C.P. No. 293
(18,201)
A.R C Technical Report

C.P. No. 293
(18 201)
A.R C Technical Report

MINISTRY OF SUPPLY

AERONAUTICAL RESEARCH COUNCIL

CURRENT PAPERS

Factors Affecting the Performance of the Nozzie of a Hypersonic Shock Tube

By

B. D Henshall, B.Sc , Ph.D.,

and

G. E. Gadd, B A., Ph D.

LONDON HER MAJESTY'S STATIONERY OFFICE

1956

Price 4s 6d net

C.P. No. 293

Factors Affecting the Performance of the Nozzle of a Hypersonic Shock Tube

- By -
B. D. Henshall B.Sc., Ph.D.
and
G. E. Gadd, B.A., Ph.D.
of the Aerodynamics Division, N.P.L.

4th February, 1956

1. SUMMARY

An analysis of the starting process of a hypersonic shock tube is made and the subsequent flow conditions in the working section are evaluated for various static temperatures and Mach numbers of the flow. A discussion of the simulation of free-flight conditions leads to recommendations for the optimum operation of hypersonic shock tubes: performance charts are given.

---

2. Introduction

The ease with which very high Mach number flows - with stagnation temperatures approximating to those of full-scale flight - may be generated in hypersonic shock tubes has led to the rapid development of this latest type of intermittent wind tunnel. However, the ultra-short duration of the steady hypersonic flow poses formidable instrumentation problems.

Reference 1 reviews the aerodynamic principles involved in the production of very strong shock waves and very high Mach number flows; a brief recapitulation of the main features of the flow pattern occurring in the channel of a hypersonic shock tube is given below. Let us consider the distance-time diagram of Figure 1. The supersonic flow behind the strong shock wave M_{S_8}* is expanded in a divergent nozzle. If $p_8 = p_1$, then the strength of the primary shock wave will decrease during its passage through the divergent section - in an analogous manner to the decay of a cylindrical blast wave - and a secondary shock wave of increasing strength will be formed by the continuous diffraction of the primary shock through the divergent channel. (For a complete account of this flow process see Ref.7.) In general, a secondary contact surface C_2 or contact region of entropy gradients will also be formed in the diffraction process; both this and the secondary upstream facing shock wave M_{S_4} will be swept downstream after the primary downstream - facing shock wave M_{S_1}. A region of steady flow at a high Mach number M_4 is established in the hypersonic working section until the arrival of the primary contact surface C_6. It is possible, if the expansion ratio of the nozzle is sufficiently large, for the strength of the shock M_{S_4} to be such that it becomes stationary with respect to the walls of the shock tube, that is $|M_{S_4}| = M_4$: it is then equivalent to the standing shock observed in a steady nozzle flow with too high a back pressure.

If/

---

*It is convenient to 'label' shock waves with their shock Mach number M_S - see Appendix for Notation.

Printed with permission of the Director, National Physical Laboratory.

If $p_8 \neq p_1$, that is, if a nozzle diaphragm is used, the Mach numbers of the transmitted shock M_{s_1} and of the secondary shock M_{s_4} are functions of the pressure ratio p_8/p_1 across the nozzle diaphragm. In the following analysis the influence of the ratio p_8/p_1 on the starting process of the nozzle flow in a hypersonic shock tube will be evaluated.

Let us consider Figure 1 and note that the primary contact surface C_6 reaches the upstream end of the hypersonic nozzle at a time τ after the incident shock M_{s_8} has reached it. Reference 1 shows that this time τ is extremely short and the time τ_R for which there is steady hypersonic flow in the nozzle working section (the running time) is even shorter.

Let the starting time τ_s be the time taken for the secondary shock wave M_{s_4} to travel through the divergent nozzle and let τ_c be the time taken by the primary contact surface C_6 to do likewise. Then the running time τ_R is given by

$$\tau_R = \tau - (\tau_s - \tau_c). \qquad \ldots\ldots(2.1)$$

For a given shock tube τ is a function of M_{s_8} only[1], and $(\tau_s - \tau_c)$ is a function of the pressure ratio p_8/p_1 across the nozzle diaphragm.

3. The Starting Process of a Hypersonic Shock Tunnel[+]

3.1 Analysis of the problem

In order to investigate the starting process in greater detail, it is necessary to determine the shock Mach numbers of the transmitted and secondary shock waves for given conditions at the entry to the nozzle and in the working section. Thus, referring to Fig.1, M_{s_1} and M_{s_4} must be determined in terms of M_{s_8} and p_8/p_1 for various values of M_4 and T_4. It is assumed that the temperature on both sides of the nozzle diaphragm is initially atmospheric ($T_1 = T_8 = 288°K$).

3.1.1. Variation of the area ratio A_4/A_6 with working section Mach number M_4 and temperature T_4

The flow at Mach number M_6, which is generated behind the primary shock in the straight tube, becomes accelerated to a Mach number M_4 after passage through the divergent nozzle. For a given area ratio A_4/A_6, M_4 depends only on M_6 and is independent of T_6 as with conventional high speed wind tunnels. If the primary shock M_{s_8} is strong, M_6 asymptotically approaches the limiting value 1.89 for infinite shock strength, and large variations in shock strength produce only small variations in M_6 (although large variations of T_6 occur). Accordingly if the area ratio A_4/A_6 is fixed, the working section Mach number is approximately independent of shock strength if the shock strength is large. This is also true with shocks of moderate strength as the following analysis shows:-

From/

[+]Shock tubes which are designed to produce a hypersonic flow of ultra-short duration are frequently referred to as 'impulse tunnels' or 'shock tunnels'.

From isentropic flow theory, if $\gamma = 1.4$,

$$\frac{T_6}{T_4} = \frac{1 + 0.2M_4^2}{1 + 0.2M_6^2} = \left(\frac{a_6}{a_4}\right)^2 = \left(\frac{\rho_6}{\rho_4}\right)^{\frac{1}{2.5}} = \left(\frac{p_6}{p_4}\right)^{\frac{1}{3.5}} \quad \ldots.(3.1)$$

and

$$\frac{A_4}{A_6} = \frac{\rho_6\, a_6\, M_6}{\rho_4\, a_4\, M_4} = \frac{M_6}{M_4}\left(\frac{T_6}{T_4}\right)^3 . \quad \ldots.(3.2)$$

If $T_6 = 288°K$, M_4 is given by

$$M_4 = \left[5\left\{\frac{288}{T_4}(1 + 0.2M_6^2)\frac{T_6}{T_6} - 1\right\}\right]^{\frac{1}{2}} . \quad \ldots.(3.3)$$

From simple shock tube theory[2] M_6 and T_6/T_6 are functions of the primary shock Mach number M_{s6} and are given by the equations

$$M_6 = \frac{5(M_{s6}^2 - 1)}{\sqrt{(7M_{s6}^2 - 1)(5 + M_{s6}^2)}} \quad \ldots.(3.4)$$

$$\frac{T_6}{T_6} = \frac{(7M_{s6}^2 - 1)(5 + M_{s6}^2)}{36\, M_{s6}^2} . \quad \ldots.(3.5)$$

Table I presents values of M_4 and A_4/A_6 for various values of M_{s6} and T_4, calculated from (3.1) to (3.5). The numerical suffices to (M_4) and (A_4/A_6) are the values of T_4 in °K, and thus $(M_4)_{150}$ denotes M_4 when $T_4 = 150°K$. Note that if $M_6 < 1$, a nozzle which first contracts to a throat would be required to produce the supersonic flow at a Mach number M_4. The corresponding tabular values are not of practical interest, but are useful in plotting M_4 as a function of A_4/A_6 as in Figure 2. As stated above the relation between the test section Mach number M_4 and the area ratio A_4/A_6 is approximately unique and independent of the working section temperature T_4. This is a most useful result, since it means that if a particular Mach number M_4 is desired and the appropriate area ratio A_4/A_6 for the nozzle is chosen from Fig.2, substantially the same Mach number M_4 will be obtained even if, due to experimental imperfections, the primary shock Mach number M_{s6} is considerably different from its expected value. The values of the temperature T_4 and pressure p_4 in the working section will, however, be approximately proportional to T_6 and p_6 and thus will be affected by errors in the shock Mach number M_{s6}.

Hence, for a given shock tube with A_4/A_6 fixed, M_4 is fixed; however, T_4 may be varied by alteration of M_{s6}.

Figures 3 and 4 present results calculated from equations (3.3), (3.4) and (3.5) and illustrate the variation of Mach number M_4 and static temperature T_4 in the working section with incident shock Mach number M_{s6}.

3.1.2. Determination of shock velocities

The solution of the equations governing the passage of the shocks through the expanding nozzle presents considerable difficulties, but when the shocks have passed out of the expansion into the parallel working section their velocities are readily calculable. Let us refer to Fig.1, where both shocks are proceeding with uniform velocities

along/

along the hypersonic channel. From the Rankine Hugoniot equations for the downstream-facing shock M_{s_1}

$$\frac{p_2}{p_1} = \frac{2\gamma}{\gamma+1} M_{s_1}^2 - \frac{\gamma-1}{\gamma+1}, \qquad \ldots.(3.6)$$

and

$$\frac{u_2}{a_1} = \frac{2}{\gamma+1}\left[M_{s_1} - \frac{1}{M_{s_1}}\right]. \qquad \ldots.(3.7)$$

Also, for the upstream-facing shock M_{s_4}, where M_{s_4} is defined

by

$$M_{s_4} = \frac{u_4 - U_4}{a_4} \qquad \ldots.(3.8)$$

and U_4 is the shock velocity relative to the tube,

$$\frac{p_3}{p_4} = \frac{2\gamma}{\gamma+1} M_{s_4}^2 - \frac{\gamma-1}{\gamma+1} \qquad \ldots.(3.9)$$

and

$$\frac{u_4-u_3}{a_4} = \frac{2}{\gamma+1}\left[M_{s_4} - \frac{1}{M_{s_4}}\right]. \qquad \ldots.(3.10)$$

Note that in the regions 2 and 3 (between the shocks M_{s_1} and M_{s_4}), $p_2 = p_3$ and $u_2 = u_3$.

From (3.6) and (3.9), with $\gamma = 1.4$, we have

$$\frac{p_3}{p_1} = \left\{\frac{7M_{s_1}^2 - 1}{7M_{s_4}^2 - 1}\right\} \frac{p_3}{p_4} \qquad \ldots.(3.11)$$

and from (3.7) and (3.10), with $\gamma = 1.4$,

$$\frac{a_4}{a_1} = \left(\frac{M_{s_1}^2 - 1}{M_{s_1}}\right) \Big/ \left\{1.2\, M_4 - \left(\frac{M_{s_4}^2 - 1}{M_{s_4}}\right)\right\}. \qquad \ldots.(3.12)$$

From (3.12) it follows that

$$M_{s_1} = \tfrac{1}{2}\left(B + \sqrt{B^2 + 4}\right) \qquad \ldots.(3.13)$$

where

$$B = \frac{a_4}{a_1}\left\{1.2\, M_4 - \left(\frac{M_{s_4}^2 - 1}{M_{s_4}}\right)\right\}. \qquad \ldots.(3.14)$$

Now

$$\frac{a_4}{a_1} = \sqrt{\frac{T_4}{288}}, \quad \text{since} \quad T_3 = T_1 = 288^\circ K, \qquad \ldots.(3.15)$$

and/

and $$\frac{p_8}{p_4} = \frac{p_8}{p_6} \cdot \frac{p_6}{p_4} = \left\{\frac{6}{7M_{s_8}^2 - 1}\right\}\left\{\frac{1 + 0.2\,M_4^2}{1 + 0.2\,M_6^2}\right\}^{3.5} .$$

It follows that

$$\frac{p_8}{p_1} = \left\{\frac{7M_{s_1}^2 - 1}{7M_{s_8}^2 - 1}\right\}\left\{\frac{6}{7M_{s_4}^2 - 1}\right\}\left\{\frac{1 + 0.2\,M_4^2}{1 + 0.2\,M_6^2}\right\}^{3.5} \quad \ldots\ldots(3.16)$$

The variation of M_{s_1} and p_8/p_1 may now be determined for any combination of the working section variables M_4 and T_4. Given M_4 and T_4, B is calculated from (3.14) and hence M_{s_1} from (3.13) for a range of values of M_{s_4}. Then from Figure 3 or Figure 4 the value of M_{s_8} which corresponds to the given values of M_4 and T_4 is read off and furthermore, the variation of M_6 with M_{s_8} is known from equation (3.4). Hence p_8/p_1 is calculable from (3.16) for the given M_4 and T_4 and the corresponding M_{s_1} M_{s_4} and M_{s_8} values. Calculations were made for a series of hypersonic flow Mach numbers M_4 up to 30 with free stream static temperatures T_4 between 50°K and 550°K, and the results are presented as Figures 5 to 9 inclusive.

3.2 Discussion of the solution

The starting time τ_s, which is the time taken for the upstream-facing secondary shock wave M_{s_4} to travel through the divergent portion of the nozzle, will be a minimum when the shock M_{s_4} becomes a sound wave, ($M_{s_4} = 1$), and is swept through the nozzle with a variable velocity $(u - a)$, where u and a are local values.

When $p_8 = p_1$, shock M_{s_4} will have a finite strength; however if $p_8 \neq p_1$, it is possible to choose the value of p_8/p_1 for any given working section conditions M_4 and T_4 in order to make $M_{s_4} = 1$. Figure 7 illustrates how p_8/p_1 varies with M_4 and T_4 for the special case $M_{s_4} = 1$; these curves for $M_{s_4} = 1$ are defined as 'perfect' start curves, since they correspond to the minimum starting time. If p_8/p_1 is reduced below the value required for perfect starting M_{s_4} becomes greater than unity; specimen calculations for the case $M_4 = 15$ and variable T_4 are presented in Figure 8. When $M_{s_4} = M_1$, the shock becomes stationary with respect to the walls of the shock tube - see equation (3.8) - and if p_8/p_1 is still further reduced a stationary shock will occur in the divergent portion of the nozzle.

If p_8/p_1 is greater than the value required for perfect starting, an expansion wave will occur instead of the shock wave M_{s_4}. This feature does not improve the starting process since the head of an expansion wave travels at sonic speed in any case. Figures 5 and 6 give the corresponding values of the transmitted shock Mach number M_{s_1} for the p_8/p_1 results given in Figures 7 and 8. It will be noted from Figure 9 that the transmitted shock M_{s_1} travels faster than the corresponding incident shock M_{s_8} for perfect starting approximately according to the formula, $M_{s_1} = 1.54\,M_{s_8}$ for all M_4 and T_4 values considered.

Figures/

Figures 7 and 8 show that the pressure ratio across the nozzle diaphragm p_8/p_1 is not affected significantly by changes of T_4; it follows from Figure 2 that, for given values of A_4/A_6 and p_8/p_1, M_{s_4} (like M_4) is approximately independent of M_{s_8}.

3.3 Evaluation of the testing time losses

3.3.1. *Perfect starting*

It has been noted that the shock M_{s_4} (= 1) travels through the nozzle with a speed (u - a) where u and a are local values. Then, approximately, if N is the nozzle length,

$$\tau_s = \frac{N}{(u-a)_{mean}} = \frac{N}{\bar{a}(\bar{M}-1)} . \qquad \ldots.(3.17)$$

Further, any disturbance due to the arrival of the primary contact surface C_6 at the nozzle will travel through the nozzle with velocity (u + a) where u and a are local values. Then, approximately

$$\tau_c = \frac{N}{(u+a)_{mean}} = \frac{N}{\bar{a}(\bar{M}+1)} . \qquad \ldots.(3.18)$$

From equation (2.1), the nett total loss in testing time $\tau_L = (\tau_s - \tau_c)$,

Hence
$$\tau_L = \frac{2N}{\bar{a}} \left(\frac{1}{\bar{M}^2-1} \right) . \qquad \ldots.(3.19)$$

From specimen calculations for simple straight walled nozzles it is reasonable to put

$$\bar{a} = \frac{3}{4} a_4 \quad \text{and} \quad \bar{M} = \frac{3}{4} M_4$$

where a_4 and M_4 describe conditions in the working section.

It follows that

$$\tau_L = \frac{648\ N}{(9M_4^2-16)\sqrt{T_4}} \text{ milliseconds} \qquad \ldots.(3.20)$$

or, if $M_4 >> 1$

$$\tau_L = \frac{72\ N}{M_4^2\sqrt{T_4}} \text{ milliseconds} \qquad \ldots.(3.21)$$

where N is in feet and T_4 in °K.

3.3.2. *Non-perfect starting*

By a similar analysis to the above section, and the use of the assumption that

$$\tau_s = \frac{N}{\bar{a}(\bar{M}-M_{s_4})} = \frac{N}{\bar{a}(3M_4-4M_{s_4})}$$

it/

it follows that

$$\tau_L = \frac{324\ N}{\sqrt{T_4}} \left[\frac{1 + M_{S_4}}{(3M_4 - 4M_{S_4})(3M_4 + 4)} \right] \text{ milliseconds} \qquad \ldots\ldots(3.22)$$

Note that this is probably an overestimate of τ_L since $M_{S_4} = \frac{3}{4} M_4$ gives $\tau_L = \infty$ whereas $M_{S_4} = M_4$ should correspond to $\tau_L = \infty$. If $M_4 \gg 1$, then (3.22) becomes

$$\tau_L = \frac{108\ N}{M_4\sqrt{T_4}} \left[\frac{1 + M_{S_4}}{3M_4 - 4M_{S_4}} \right] \text{ milliseconds} \qquad \ldots\ldots(3.23)$$

3.3.3. Nozzle length

For given entry conditions the length N of a nozzle designed to produce uniform flow at the exit increases as the exit flow Mach number is raised.

An empirical relation, based on an extrapolation of results obtained at N.P.L.[6], is ($M_4 \gg 1$)

$$\frac{N}{A_4} \simeq \frac{9M_4}{10} \qquad \ldots\ldots(3.24)$$

where for a two-dimensional nozzle A_4 is the height of the working section.

Hence, for hypersonic Mach numbers, (3.21) and (3.23) become

$$\tau_L = \frac{64.8}{M_4\sqrt{T_4}} \cdot A_4 \text{ milliseconds} \qquad \ldots\ldots(3.25)$$

for a 'perfect start' and

$$\tau_L = \frac{97.2}{\sqrt{T_4}} \left[\frac{1 + M_{S_4}}{3M_4 - 4M_{S_4}} \right] A_4 \text{ milliseconds} \qquad \ldots\ldots(3.26)$$

for a non-perfect start.

Since the slope of the characteristics at hypersonic speeds is very small, the model would normally be placed approximately halfway along the nozzle. Thus (3.25) and (3.26) probably overestimate τ_L by a factor of about 2 and more realistic estimates of the nett total loss in testing time τ_L per foot of working section height would be

(Perfect start) $$\tau_L = \frac{32.4}{M_4\sqrt{T_4}} A_4 \text{ milliseconds} \qquad \ldots\ldots(3.27)$$

(Non-perfect start) $$\tau_L = \frac{48.6}{\sqrt{T_4}} \left[\frac{1 + M_{S_4}}{3M_4 - 4M_{S_4}} \right] A_4 \text{ milliseconds} \qquad \ldots\ldots(3.28)$$

where A_4 is in feet and T_4 in °K.

Calculations/

Calculations made from equations (3.27) and (3.28) are presented as Figures 10 and 11; the former gives the nett total loss of testing time per foot of working section height for perfect start conditions at various Mach numbers M_4 and temperatures T_4, whilst the latter illustrates the losses due to imperfect starting for the special case $M_4 = 15$ with variable T_4. For a fixed A_4 and a variable A_8 the testing time losses are greatest for low T_4 and low M_4.

4. Simulation of Free Flight Conditions in Hypersonic Shock Tubes

In the following sections the factors which affect the simulation in a shock tube of hypersonic flight at extreme altitudes are discussed.

4.1 The Reynolds number

The Reynolds number based on the length L_m of the model is

$$R_m = \frac{\rho_4 \, U_4 \, L_m}{\mu_4} .$$

If T_4 is in °K and $\mu \propto T$, then if $T_8 = 288°K$

$$R_m = \frac{\rho_4 \, M_4 \, L_m . \; 1120 \left(\frac{T_4}{288}\right)^{\frac{1}{2}}}{3.72 \times 10^{-7} \left(\frac{T_4}{288}\right)} .$$

But, if $\gamma = 1.4$, equation (3.1) yields

$$\rho_4 = \rho_8 \left(\frac{T_4}{T_6}\right)^{2.5} = 0.00238 \, \frac{\rho_8}{\rho_8} . \frac{p_8}{p_6} . P \left(\frac{T_4}{288 \, \frac{T_6}{T_8}}\right)^{2.5}$$

where $P = p_8$ (measured in atmospheres)

and $\rho_8 = 0.00238 \, \frac{\rho_8}{p_8} . P$ slugs/cu ft.

Now $\frac{p_8}{p_8} . \frac{\rho_6}{\rho_8} = \frac{T_8}{T_6}$ and using (3.1) we get

$$R_m = \frac{7.15 \times 10^6}{(1+0.2M_4^2)^2} . P.M_4 \, L_m . G \qquad .....(4.1)$$

where

$$G = (1 + 0.2 \, M_8^2)^2 . \left(\frac{T_8}{T_6}\right)^{\frac{3}{2}} \qquad .....(4.2)$$

and L_m is measured in feet.

Clearly G is a function of the primary shock Mach number M_{s_8} only and specimen values are given below.

TABLE 2

M_{s_8}	2	4	6	8	10	12	14	16	18	20
G	0.752	0.272	0.115	0.055	0.030	0.018	0.0117	0.0078	0.0056	0.0042
$G\frac{p_6}{p_8}$	3.38	5.02	4.82	4.10	3.50	3.06	2.68	2.32	2.11	1.95

Let/

Let us assume that the maximum pressure in the channel $p_8 = P$ atmospheres, independent of M_{s_8}, and governed only by the tube construction. Then for a given M_4, the Reynolds number R_m is proportional to G and the value of p_8 is so chosen that $\frac{p_6}{p_8} \cdot p_8 = P$ atmospheres for each M_{s_8}.

Hence for maximum Reynolds numbers the tube must be operated so that GP is a maximum; that is, the lowest possible shock Mach number M_{s_8} must be used. Now suppose that the actual M_{s_8} achieved in an experiment is less than the value expected; then R_m is proportional to $GP.\frac{p_6}{p_8}$. Table 2 shows that $G\frac{p_6}{p_8}$ decreases slowly as M_{s_8} increases; hence if M_{s_8} is less than expected, the Reynolds number will be slightly greater than expected.

This important result - that the lowest values of M_{s_8} give the highest Reynolds numbers - is subject to the limitation that the static temperature T_4 in the working section must not be allowed to become less than the temperature at which air liquefies. This critical temperature, a function of the pressure p_4 in the working section, is given by the following approximate relation obtained by extrapolation of the data given in Ref.3,(p.406).

$$\log_{10} p_4 = \log_{10} \frac{p_4}{p_6} \cdot P = 4.4 - \frac{360}{T_4} \qquad \ldots\ldots(4.3)$$

where T_4 is measured in °K and P in atmospheres.

Now $\frac{p_4}{p_6} = \left(\frac{1+0.2M_6^2}{1+0.2M_4^2}\right)^{3.5}$ and since for any $M_{s_8} > 4$ we have $1.48 < 1 + 0.2M_6^2 < 1.71$, the ratio $\frac{p_4}{p_6}$ is approximately a function of M_4 only.

Thus, to avoid liquefaction,

$$T_4 > \frac{360}{4.4 + 3.5 \log_{10}\left\{\frac{1+0.2M_4^2}{1+0.2M_6^2}\right\} - \log_{10} P} \cdot \qquad \ldots\ldots(4.4)$$

Table 3 gives values of the liquefaction temperature calculated from equation (4.4) for the two extreme cases of P = 1 and P = 500 atmospheres. (The factor $(1 + 0.2\ M_6^2)$ in equation (4.4) is replaced by 1.71, its approximate value for all large values of M_{s_8}.)

TABLE 3

M_4	10	14	18	22	26	30
T_4 °K(P = 500 atm)	65	56	49	46	43	41
T_4 °K(P = 1 atm)	44	40	36	34	33	31

Hence, to avoid liquefaction, T_4 must not fall below about 50°K for any hypersonic Mach number M_4.

4.2/

4.2 The equivalent altitude

The altitude at which a full-scale aircraft must fly if it is to have the same Reynolds number as a scale model in a hypersonic shock tube is now determined. The temperature in the stratosphere between 40,000 and 100,000 feet is usually assumed constant and equal to 216.5°K. At extreme altitudes the temperature is greater than 216.5°K; but this increase appears to be small, particularly during winter and during night time in summer. Hence it is assumed that $T = 216.5°K$ for all altitudes greater than 40,000 feet. The density of the atmosphere then decreases exponentially with the altitude (h feet) according to the approximate relation

$$\rho = 0.0040e^{-4.8 \times 10^{-5} h} \text{ slugs/cu ft.} \qquad \ldots\ldots(4.5)$$

Now if the full-scale aircraft is n times as large as the model it follows that, for equal Reynolds numbers

$$\left(\frac{\rho U}{\mu}\right)_{4, \text{shock tube}} = n \left(\frac{\rho U}{\mu}\right)_{n, \text{flight}} . \qquad \ldots\ldots(4.6)$$

If equal model and full-scale Mach numbers are assumed it can be shown, by an analysis similar to that leading to equation (4.1), that

$$h + 4.8 \times 10^4 \log_{10} \frac{P}{n} = 4.8 \times 10^4 \log_{10} \left\{ \frac{1.9(1+0.2M_4^2)^2}{G} \right\} \qquad \ldots\ldots(4.7)$$

where $P = p_6$ (atmospheres) - shock tube and the variation of G with M_{s_8} is given by Table 2. An alternative form for (4.7) is

$$h + 2.1 \times 10^4 \log_e \frac{P}{n} = 2.1 \times 10^4 \log_e \left\{ \frac{1.6 \times 10^5}{T_4^2} \left(\frac{T_6}{T_8}\right)^{3.5} \right\} . \qquad \ldots\ldots(4.8)$$

Equations (4.7) and (4.8) show that the equivalent altitude h can be reduced by making P large or n small. Nevertheless, it would be necessary to use impracticably large pressures and large models in the shock tube in order to simulate a large aircraft moving (say) at a Mach number of 20 at a relatively low altitude - say 50,000 feet. Fortunately such aircraft are likely to operate only at extreme altitudes. It may be useful to have an expression for the full-scale Reynolds number R, at Mach number M, under the atmospheric conditions assumed in this section. Then R is given by

$$\frac{R}{ML} = \frac{1.31 \times 10^7}{e^{4.8 \times 10^{-5} h}} \qquad \ldots\ldots(4.9)$$

where L is the length of the full-scale aircraft in feet.

4.3 Slip-flow conditions

At large equivalent altitudes and very low air densities the mean free path ℓ of the air molecules becomes large. If the ratio of ℓ to the length of the body becomes too great the air can no longer be considered as a continuum and slip flow occurs. It is of interest to examine the conditions which must be achieved in the model experiment if the onset of slip flow under full-scale conditions is to be reproduced.

Consider/

Consider the equivalent altitude, H feet, at which

$$\left(\frac{\text{Mean free path}}{\text{length of model}}\right)_4, \text{ shock tube} = \left(\frac{\text{mean free path}}{\text{length of aircraft}}\right)_H, \text{ flight} \qquad \ldots\ldots(4.10)$$

The mean free path is inversely proportional to the density and is independent of temperature. Thus, for an aircraft n times as large as the shock tube model, similarity is achieved if n is given by

$$n = \frac{\rho_4, \text{ shock tube}}{\rho_H, \text{ flight}}.$$

By an analogous analysis to that leading to equation (4.8) it follows that

$$H + 2.1 \times 10^4 \log_e \frac{P}{n} = 2.1 \times 10^4 \log_e \left\{ \frac{2.35 \times 10^6}{T_4^{2.5}} \left(\frac{T_s}{T_s}\right)^{3.5} \right\} \ldots(4.11)$$

If equations (4.8) and (4.11) are considered, it is noted that the right hand sides are functions of M_{s_s} and T_4 only (see Table 1). Calculated values of $\left(H + 2.1 \times 10^4 \log_e \frac{P}{n}\right)$ and $\left(h + 2.1 \times 10^4 \log_e \frac{P}{n}\right)$ for ranges of M_{s_s} and T_4 are presented in Figure 12.

The simple kinetic theory of gases[4] shows that the Knudson number

$$\frac{\ell}{L} = 1.5 \frac{M}{R} \qquad \ldots\ldots(4.12)$$

and hence for Reynolds number and Mach number similarity between full scale and shock tube, ℓ/L in flight at height h should be the same as in the shock tube. It follows that on this basis h and H should be identical. The reason for the small discrepancy in Fig.12 between h and H is that h has been calculated by assuming viscosity proportional to absolute temperature. This is roughly correct, but is at variance with simple kinetic theory which predicts too small a variation of viscosity with temperature. However, these small differences between h and H may be ignored.

Following Tsien[4], it is assumed that if slip flow is not to occur

$$\frac{\ell}{\delta^*} < 0.01 \qquad \ldots\ldots(4.13)$$

where ℓ is the mean free path and δ^* is the displacement thickness of the boundary layer. Since aircraft flying at very high Mach numbers are likely to be travelling at extreme altitudes, the Reynolds numbers will be low and the boundary layers laminar. If there is zero heat transfer between the free-stream air and the body (that is, if there is no radiation and the body has become heated to its equilibrium temperature) δ^* will be of the same order as the theoretical result[5] for a flat plate with zero heat transfer.

Hence $$\delta^* \doteqdot 1.72 \, (1 + 0.277 \, M^2) \frac{x}{\sqrt{R_x}}$$

which becomes, when $M \gg 1$

$$\delta^* \simeq \tfrac{1}{2} \frac{xM^2}{\sqrt{R_x}} \qquad \ldots\ldots(4.14)$$

where/

where R_x is based on x, the distance from the leading edge to the boundary-layer station under consideration. For an average value of the boundary-layer thickness along the body it is convenient to take the value at $x = \frac{1}{4}L$; this is given by

$$\delta^* \simeq \frac{M^2 L}{4\sqrt{R}} \qquad \ldots\ldots(4.15)$$

In (4.13) it is not appropriate to use ℓ as given by (4.12), since (4.12) refers to the mean free path outside the boundary layer. Within the boundary layer the air is heated and consequently the density decreases and the mean free path increases. Hence the maximum value, ℓ_{max}, of ℓ from (4.13) should be used. This is given by

$$\frac{\ell_{max}}{\ell_\infty} = \frac{T_{max}}{T_\infty} \simeq 1 + 0.2\,M^2 \simeq 0.2\,M^2$$

where ℓ_∞ and T_∞ are the mean free path and temperature in the free stream. Hence (4.12), (4.13) and (4.15) require that, if slip flow is to be avoided,

$$0.2\,M^2 . \frac{1.5M}{R} . \frac{4\sqrt{R}}{M^2} . < 0.01$$

or approximately $$R > 10^4\,M^2. \qquad \ldots\ldots(4.16)$$

It is interesting to note that (4.16) is also obtained if it is assumed that the wall temperature is much less than the zero heat transfer value. Thus if the wall temperature were equal to the free stream temperature (which would require drastic cooling) the boundary layer thickness would be reduced to about 0.25 of the insulated value, but so would the maximum temperature; hence ℓ_{max} would be reduced in the same proportion as δ^*, and the net result would be to leave ℓ_{max}/δ^* unchanged.

By substituting in (4.9) from (4.16) it can be shown that slip flow will be avoided with the full scale aircraft if

$$h < 2.1 \times 10^4 \log_e \left(1.31 \times 10^3 \frac{L}{M}\right) \qquad \ldots\ldots(4.17)$$

where h, the altitude, and L, the aircraft length, are measured in feet. In the shock tube, for a model of length L_m feet, the corresponding condition is, from (4.1) and (4.16),

$$\frac{715\ GPL_m}{M_4\ (1+0.2\,M_4^2)^2} > 1. \qquad \ldots\ldots(4.18)$$

As an example, suppose an aircraft of length 50 feet is travelling at $M = 15$. Slip flow will occur if it flies above 175,000 feet. In the shock tube, for a model of length 1 foot and $P = 500$ atmospheres, we find that G must be > 0.088 (which corresponds to $M_{s_8} < 7$ and $T_4 < 100^\circ K$ approximately) to avoid slip flow.

4.4/

4.4 Simulation of full-scale temperature conditions

In Sections 4.1 and 4.2 the problem of attaining full-scale Reynolds numbers was discussed. However, even if the Mach number and Reynolds number in the shock tube have their full-scale values, it does not necessarily follow that similarity of flow will be achieved. It is necessary also that the ratio of the body surface temperature T_s to the free-stream temperature T_∞ should be the same for the model as for the full-scale aircraft. For the aircraft, except near the nose, T_s/T_∞ is likely to be much less than the zero heat transfer value, which is approximately $0.2\ M^2$. The extent to which T_s/T_∞ falls below this value will depend on the time for which the aircraft has been flying and its heat capacity, on radiation conditions, etc. However in all conditions T_s/T_∞ is likely to be large, although much less than $0.2\ M^2$. In the shock tube, if the heat capacity and thermal conductivity of the model are both fairly large, T_s is likely to remain quite near to its value before the flow starts, except near the nose, because the flow duration is so short. Normally the initial value of T_s will be room temperature, so to get realistically large values of T_s/T_∞ it is necessary to use low free-stream temperatures T_∞ (or T_4 in our usual notation). In fact it is probably necessary to use the lowest possible value of T_4, roughly 50°K. Fortunately this will also give the highest possible Reynolds number. However it is desirable to investigate in the shock tube the effects of varying T_s/T_∞ ($\equiv T_s/T_4$) ; this can be done by preheating (or less conveniently by pre-cooling) the model or by the use of various free-stream temperatures T_4. Thus for certain experiments, it will probably be desirable to work at values of T_4 much higher than the minimum*. This will of course entail a considerable sacrifice of Reynolds number.

There is a further barrier to the attainment of complete flow similarity between the shock tube and full scale. Even if the temperature ratio T_s/T_∞ is the same as in flight the flow will not be similar if the absolute temperaturesin the full-scale condition are much greater than in the shock tube; particularly if they are so great that serious dissociation and ionisation effects occur. Such effects certainly will occur in flight at sufficiently high Mach numbers, and under these conditions complete simulation of the full-scale flow by shock tube testing is virtually impossible. However, a similar limitation has always attended the testing of models at relatively low speeds in wind tunnels. It is pertinent to point out that studies of ionisation and dissociation effects in real gas flows may be made in shock tubes and hence a further type of flow simulation is possible. In this latter case the simulation of the radiation from a heated aircraft flying at hypersonic speeds would be a very difficult problem.

5. Conclusions and Recommendations

Performance charts for the operation of hypersonic shock tubes have been developed from an evaluation of the simulation of free-flight conditions, and an analysis of the factors affecting the starting process of the shock tunnel. The use of a diaphragm at the entrance to the nozzle is shown to be imperative in order to minimise the loss of testing time due to tunnel starting; this diaphragm would normally have a pressure ratio of at least 10^4 across it. This implies that the working

section/

---

*Values greater than room temperature are, however, unlikely to be wanted since these would make $T_s/T_\infty < 1$ if T_s is equal to room temperature, and such small ratios would only be of academic interest.

section must be evacuable to an initial pressure of 1 to 0.1 microns of mercury if Reynolds number simulation of flight conditions is to be obtained in the working section during the hypersonic flow test period.

A complete calculation of the design performance of the N.P.L. hypersonic shock tube installation is deferred until a later paper; however, specimen results indicate that the testing time losses should not normally exceed 25% of the theoretical[1] testing time under normal working conditions.

From the present calculations it is clear that, to obtain Mach number and Reynolds number simulation of free flight conditions, the shock tube must be operated at low incident shock Mach numbers M_{s_8}; this implies that the free-stream temperature in the working section will be less than atmospheric (that is, the model will be hotter than the free stream as under full-scale conditions) but the stagnation temperature of the flow will be less than that of free flight. Alternatively, the correct stagnation temperature and Reynolds number conditions may be obtained in a shock tube without a nozzle; this implies that M_{s_8} should be very large, with a consequent reduction[1] of theoretical testing time and an elimination of the nozzle starting losses.

Thus hypersonic shock tubes should have two working sections; one in the constant area channel for temperature simulation and one following a divergent nozzle for Mach number simulation.

It is possible to obtain simultaneous Mach number and temperature simulation in the expanded hypersonic flow but the static temperature of the flow will be greater than the temperature of the model - an unreal condition - and furthermore it is very difficult to avoid slip flow for this case.

Thus it appears likely that the simulation of flight at hypersonic Mach numbers and extreme altitudes will be studied in the following stages in shock tube installations:

(1) Reynolds number and Mach number simulation with variable T_4/T_{model} in a divergent nozzle working section.

and (2) Reynolds number and stagnation temperature simulation (with the associated real gas effects) in a constant area working section in the channel of the shock tube.

APPENDIX/

APPENDIX

Notation

a	velocity of sound
A	cross-sectional area of shock tube
G	a function of shock Mach number - see eqn. (4.2)
h	altitude - see eqn. (4.8)
H	altitude - see eqn. (4.11)
ℓ	mean free path of a molecule
L	characteristic length
M	Mach number
$M_{()}$	flow Mach number with respect to the local speed of sound (e.g. $M_2 = u_2/a_2$)
$M_{s_{()}}$	shock wave propagation Mach number with respect to the speed of sound in the flow ahead of the shock front (e.g. $M_{s_1} = U_1/a_1$)
n	scale ratio between model and full size aircraft
N	length of nozzle section of hypersonic shock tube
p	absolute pressure
P	(= p_6, see Figure 1) absolute pressure, measured in atmospheres
R_x	Reynolds number based on length x
T	absolute temperature
u	flow velocity
U	shock velocity; subscript corresponds to flow region ahead of the shock
x	distance
γ	C_p/C_v, the ratio of the specific heats
ρ	absolute density
μ	coefficient of viscosity
τ	theoretical testing time
τ_R	tunnel running time
τ_L	nett loss of testing time due to starting process of hypersonic shock tube
δ^*	displacement thickness of boundary layer

Subscripts/

Subscripts

o	stagnation conditions
1, 2, 3, 4 .... etc	identify quantities related to gas in corresponding region of shock tube flow diagram (Figure 1)
∞	free stream conditions in full-scale flight
m	model
s	surface conditions

References

No.	Author(s)	Title, etc.
1	B. D. Henshall	Some notes on the flow durations occurring in hypersonic shock tubes A.R.C.17,608 - F.M.2243 - T.P.461 11th August, 1955.
2	B. D. Henshall	On some aspects of the use of shock tubes in aerodynamic research. University of Bristol, Department of Aeronautical Engineering, Report No.P.4. Communicated by Prof. A. R. Collar. A.R.C.17,407 - T.P.449 24th February, 1955. and Corrigendum - 13th July, 1955.
3	R. C. Pankhurst and D. W. Holder	Wind tunnel technique. Pitman, London 1952.
4	H. S. Tsien	Superaerodynamics; mechanics of rarefied gases. J.Ae.Sciences, Vol.13 p.653. 1946.
5	A. D. Young	Skin friction in the laminar boundary layer in compressible flow. Aeronautical Quarterly, Vol.1, Part II p.137 (August 1949)
6	E. W. E. Rogers and Miss B. M. Davis	Basic coordinates of some supersonic nozzle profiles for supersonic wind tunnels. NPL/Aero Note/249.
7	G. Rudinger	Wave diagrams for non-steady flow in ducts. D.Van Nostrand 1955.

TABLE 1/

TABLE 1

M_4 and A_4/A_6 as functions of M_{S8} and T_4 from equations (3.1) to (3.5) $T_8 = 288°K$, $\gamma = 1.4$

M_{S8}	1	2	4	6	8	10	12	14	16	18	20
$\frac{T_6}{T_8}$	1	1.55	4.04	7.93	13.4	20.4	28.9	39.0	50.7	64.0	78.6
M_6	0	0.96	1.55	1.73	1.79	1.83	1.85	1.86	1.87	1.87	1.88
$(M_4)_{50}$	4.88	6.92	12.9	19.0	25.0	31.2	37.3	43.0	49.8	56.0	62.1
$(M_4)_{150}$	2.14	3.56	7.24	10.8	14.4	18.0	21.4	25.0	28.6	32.2	35.9
$(M_4)_{250}$	0.87	2.37	5.41	8.3	11.0	13.8	16.6	19.4	22.1	25.0	27.8
$(M_4)_{350}$	-	1.60	4.43	6.86	9.2	11.6	14.0	16.3	18.7	21.0	23.4
$(M_4)_{450}$	-	0.95	3.75	5.96	8.1	10.2	12.3	14.4	16.4	18.5	20.6
$(M_4)_{550}$	-	-	3.26	5.30	7.24	9.2	11.0	13.0	14.8	16.7	18.6
$\left(\frac{A_4}{A_6}\right)_{50}$	0	98	1,500	8,630	33,000	94,500	228,000	493,000	Very large		
$\left(\frac{A_4}{A_6}\right)_{150}$	0	7.1	99	562	2,110	6,120	14,800	31,200	60,200	108,000	180,000
$\left(\frac{A_4}{A_6}\right)_{250}$	0	2.30	28.7	159	599	1,720	4,120	8,750	16,800	29,900	50,000
$\left(\frac{A_4}{A_6}\right)_{350}$	-	1.09	12.9	70.1	260	748	1,780	3,780	7,310	13,000	21,800
$\left(\frac{A_4}{A_6}\right)_{450}$	-	0.98	7.1	37.6	139	397	955	1,980	3,860	6,950	11,550
$\left(\frac{A_4}{A_6}\right)_{550}$	-	-	4.5	23.4	85	244	578	1,300	2,380	4,220	7,380

HBD

FIG. 1.

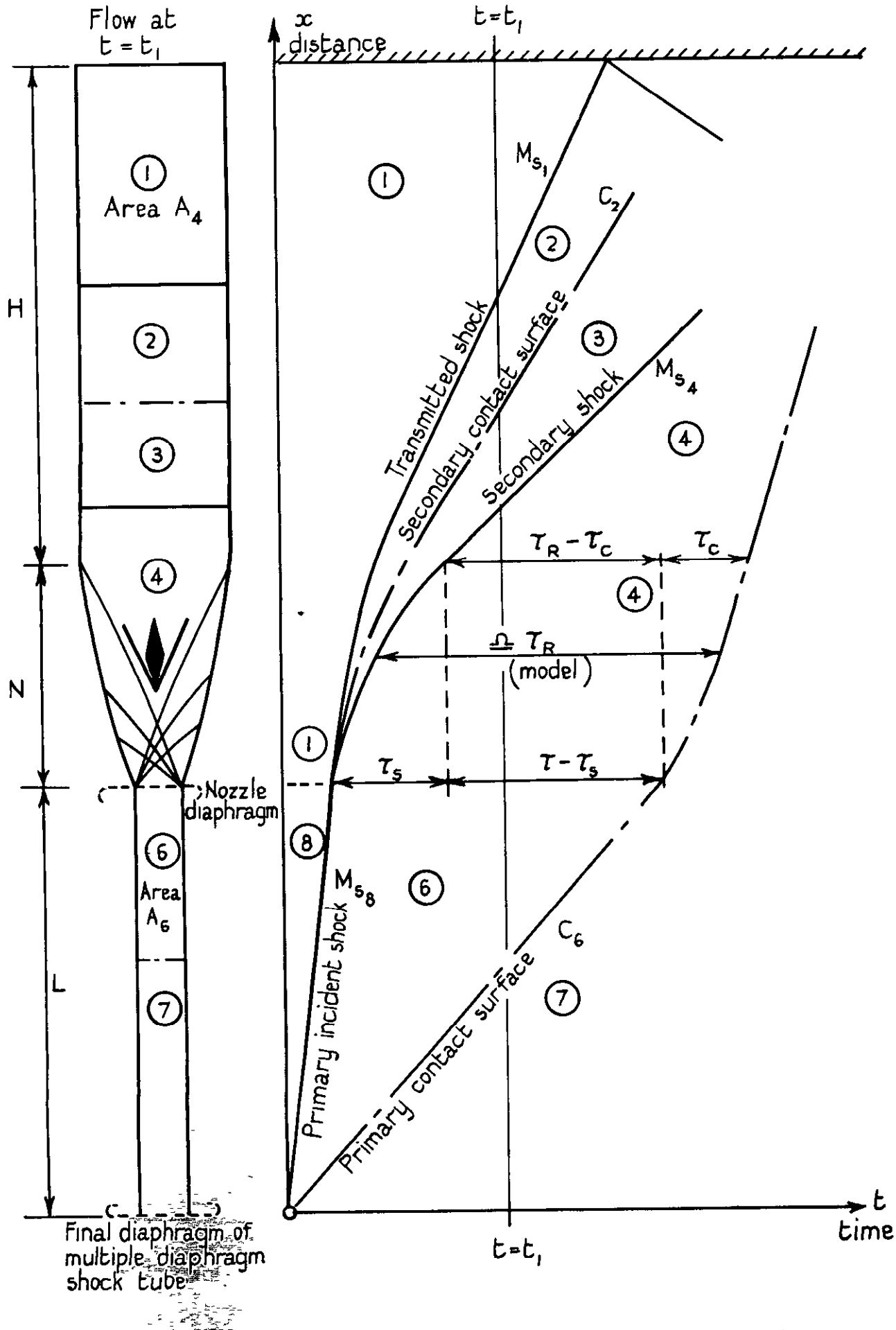

The flow in the channel of a hypersonic shock tube

FIG 2.

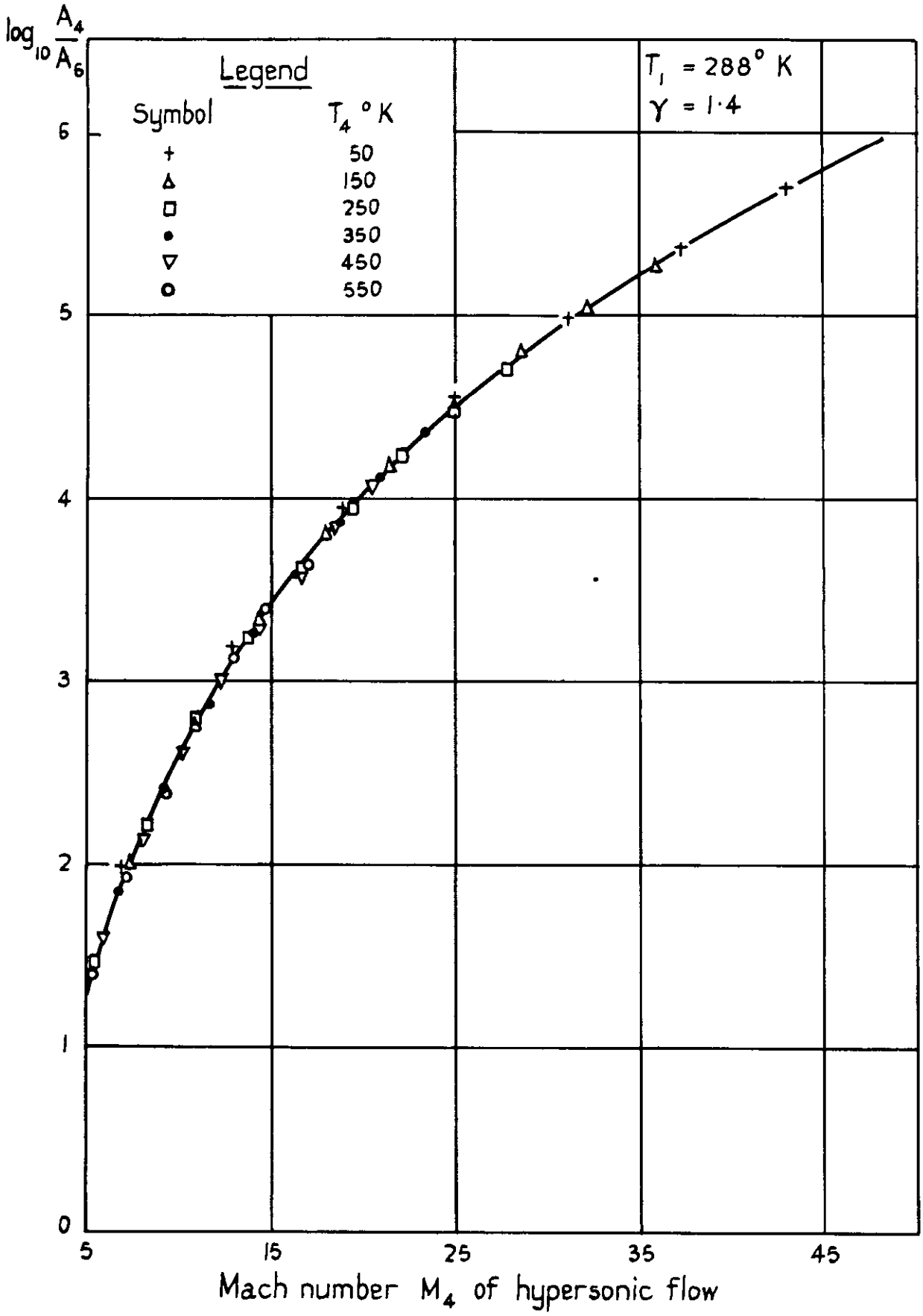

Hypersonic shock tube:

Nozzle area ratio required to produce hypersonic Mach number flows

FIG. 3.

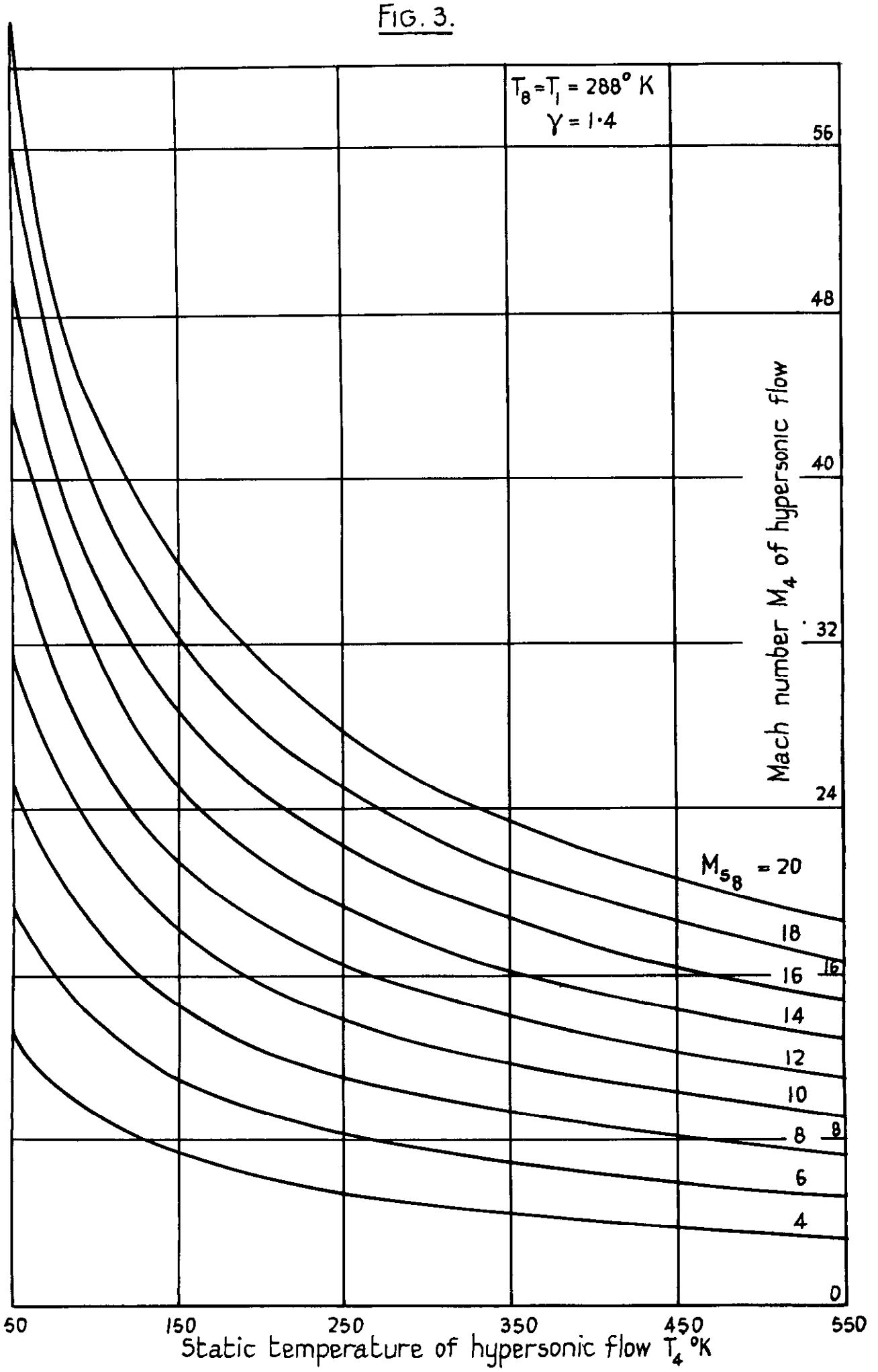

Hypersonic shock tube:
Variation of working section conditions with incident shock Mach number M_{s_8}

FIG 4.

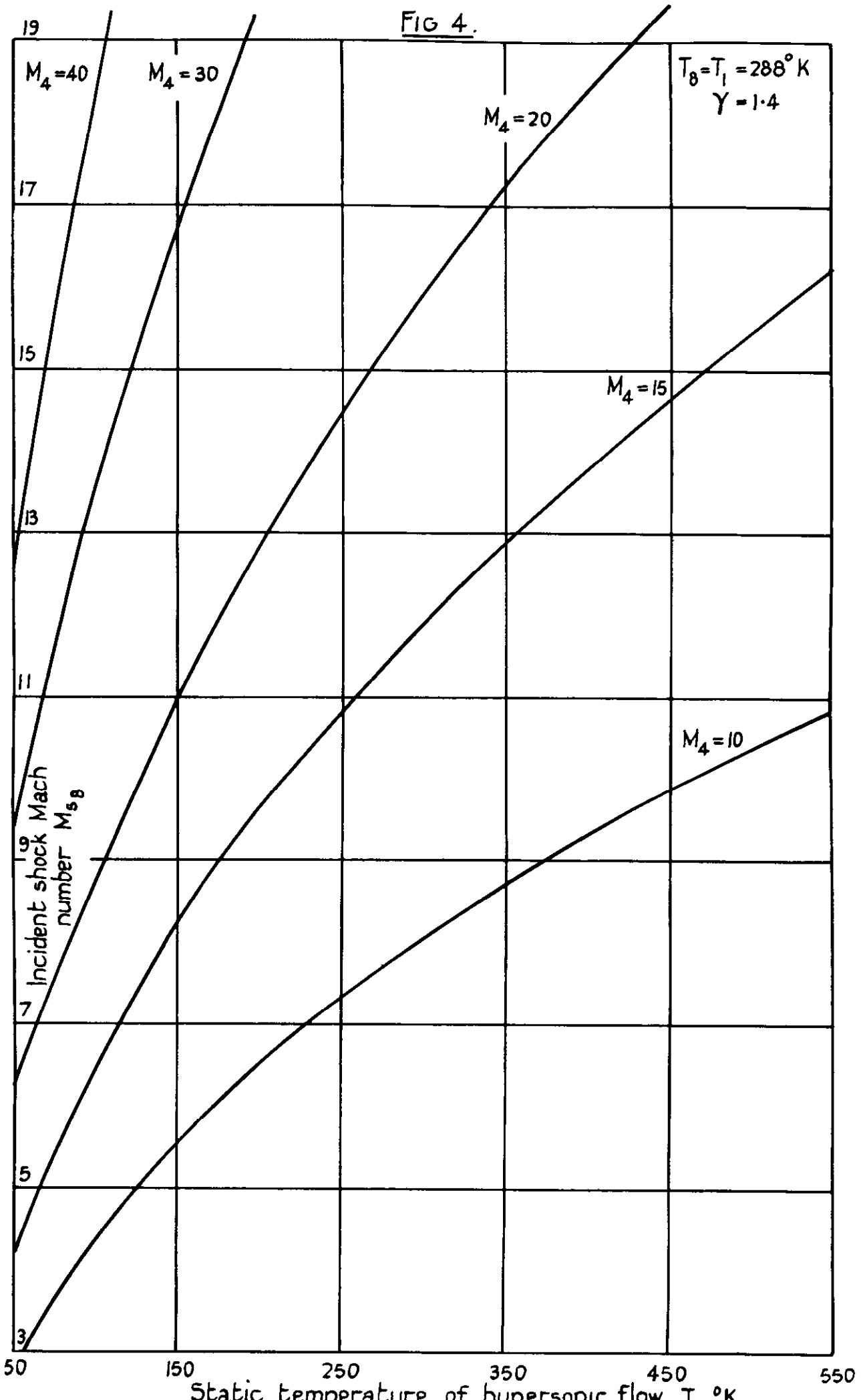

Hypersonic shock tube:
Variation of working section conditions with incident shock Mach number M_{s8}

FIG. 5.

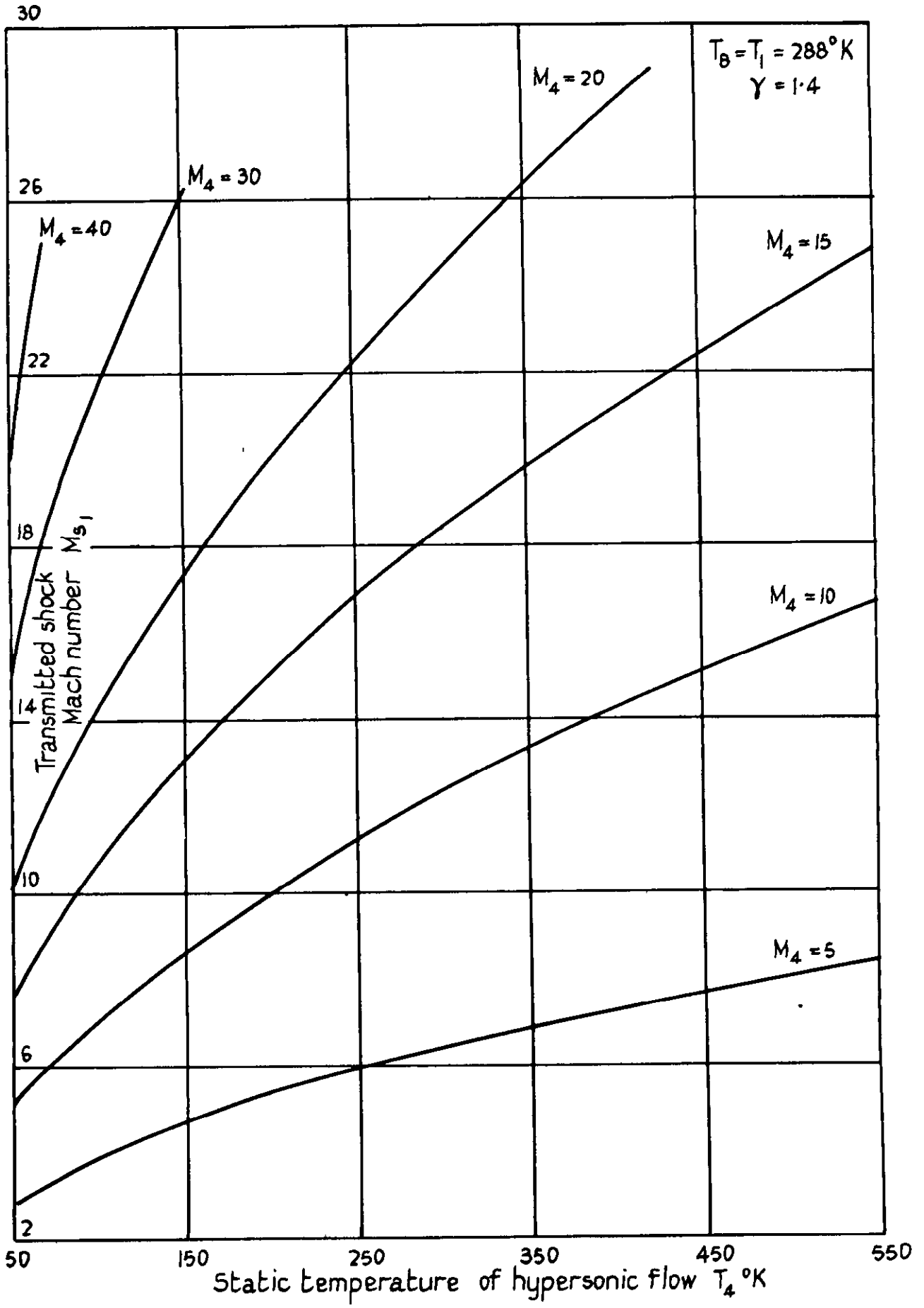

Hypersonic shock tube:
Nozzle starting process:
Transmitted shock Mach number M_{s_1}
'Perfect start' with $M_{s_4} = 1{\cdot}0$

FIG. 6.

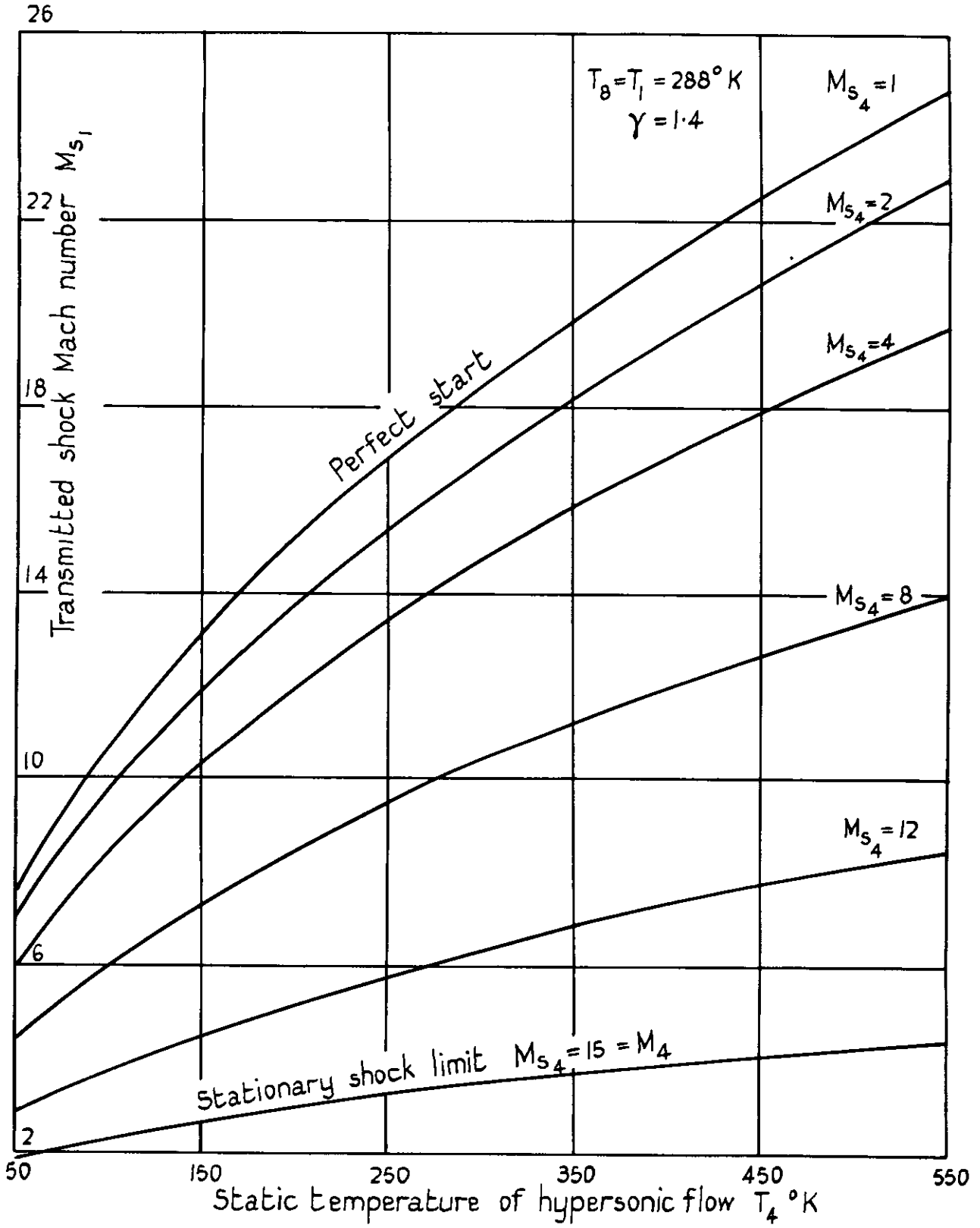

Hypersonic shock tube:
Nozzle starting process.
Transmitted shock Mach number M_{s_1}
Imperfect start:– $M_4 = 15$

FIG. 7

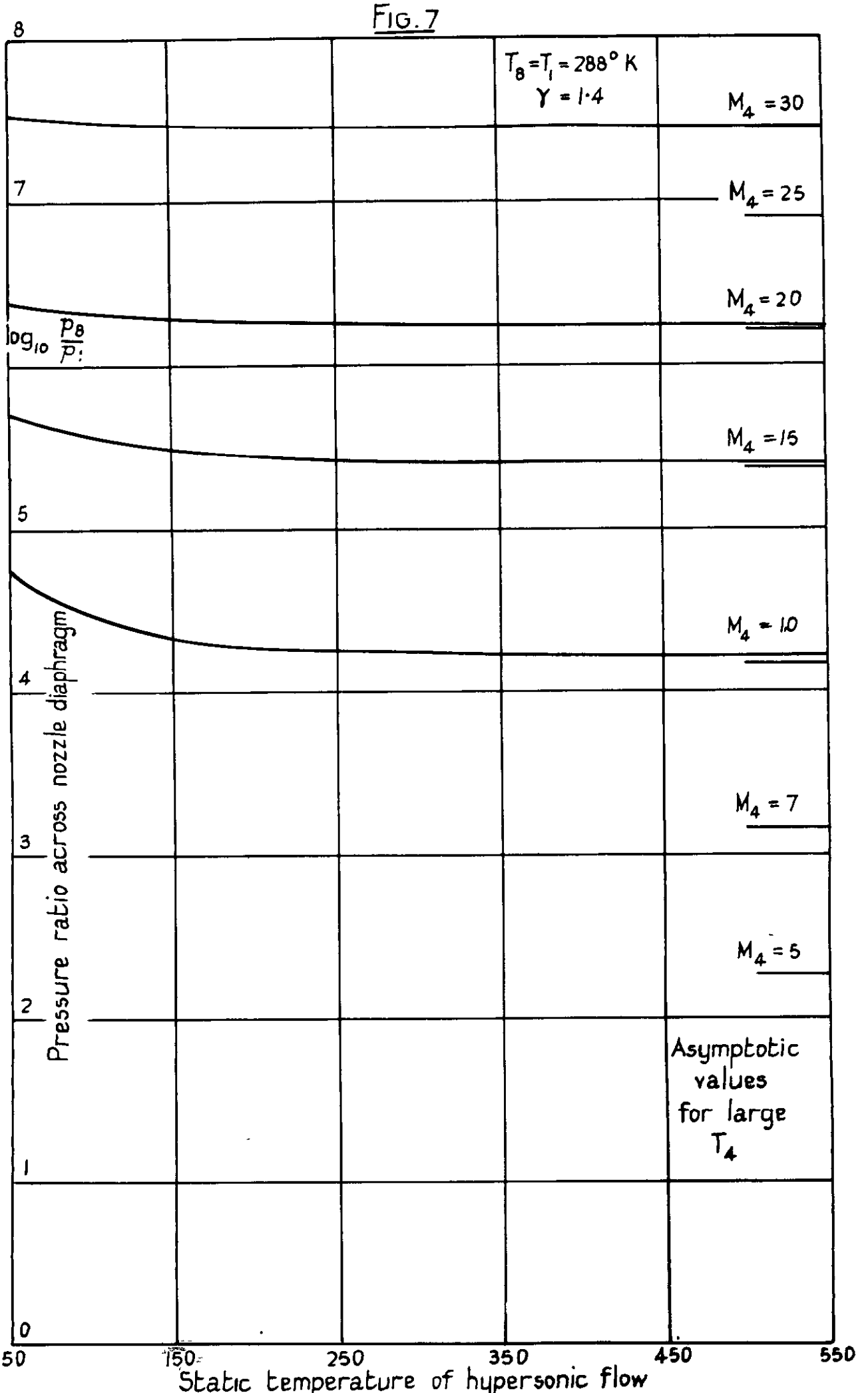

Hypersonic shock tube: Nozzle starting process: pressure ratio p_8/p_1
Perfect starting $M_{s_4} = 1$

FIG. 8.

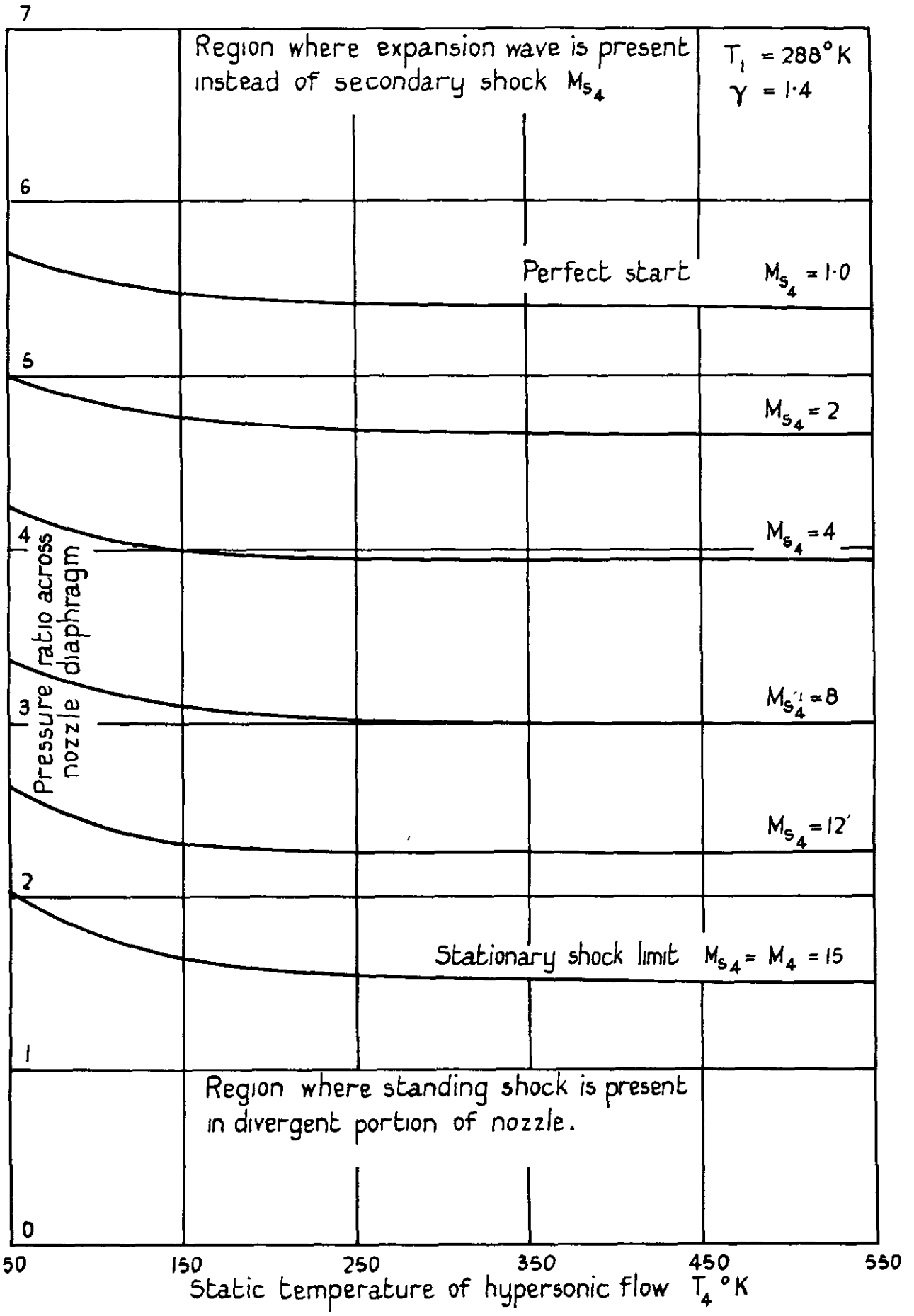

Hypersonic shock tube:
Nozzle starting process: pressure ratio p_8/p_1
Imperfect starting $M_4 = 15$

FIG. 9.

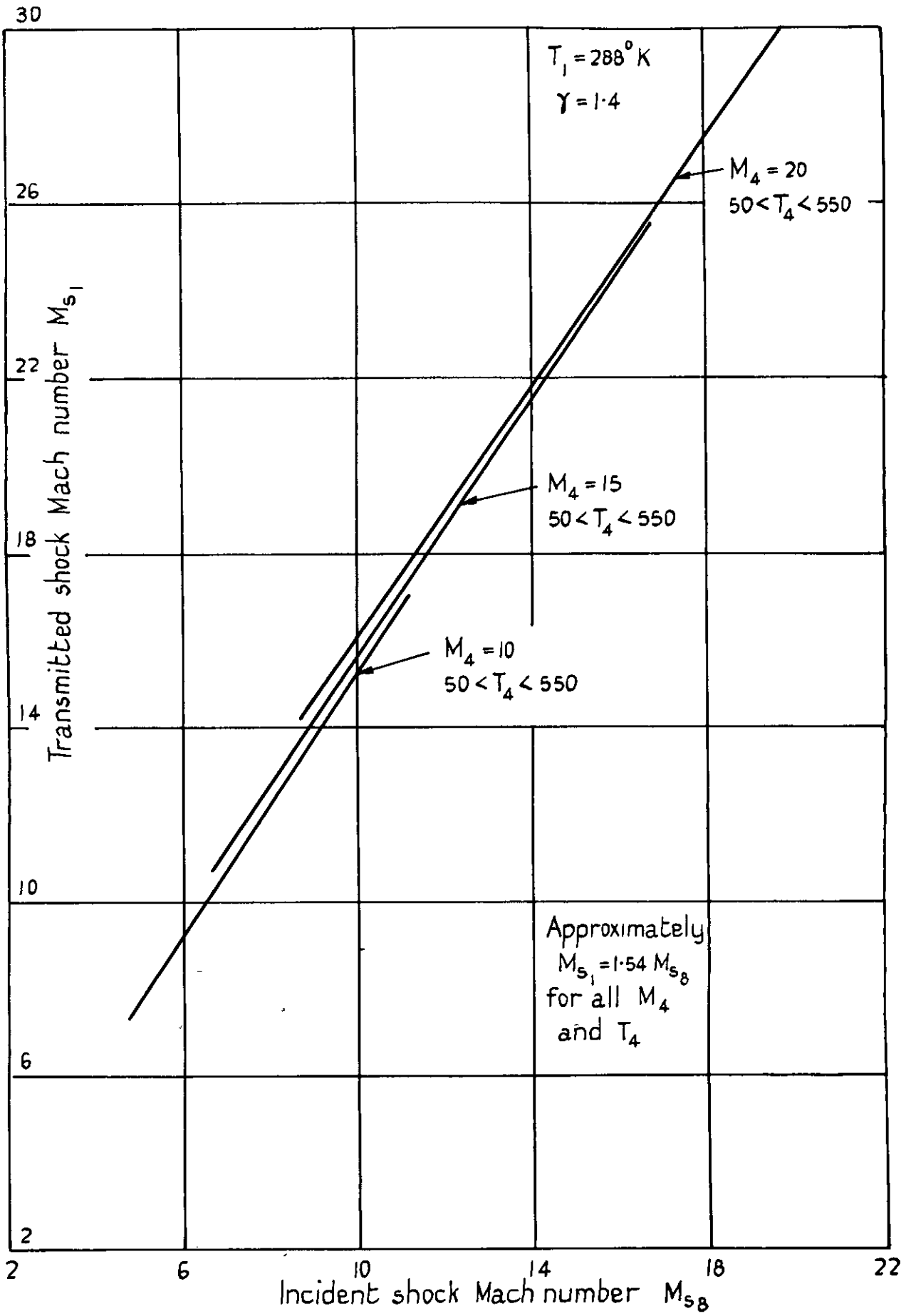

Hypersonic shock tube:
Nozzle starting process. Incident and transmitted shock Mach numbers
Perfect starting $M_{s_4} = 1$.

FIG. 10.

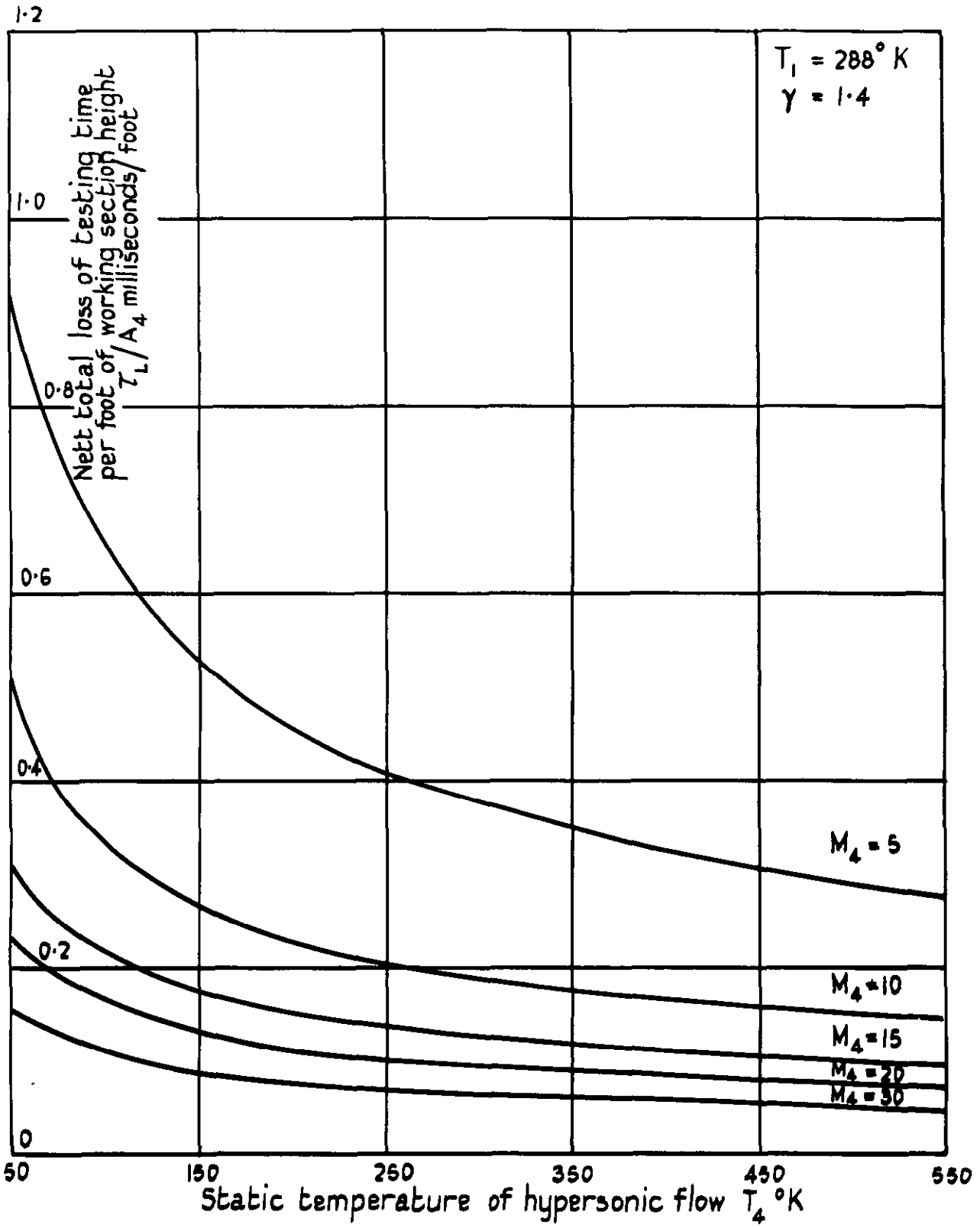

Hypersonic shock tube:
Loss of testing time due to starting process
Perfect start $M_{s_4} = 1.0$
(Two-dimensional nozzle).

FIG. 11

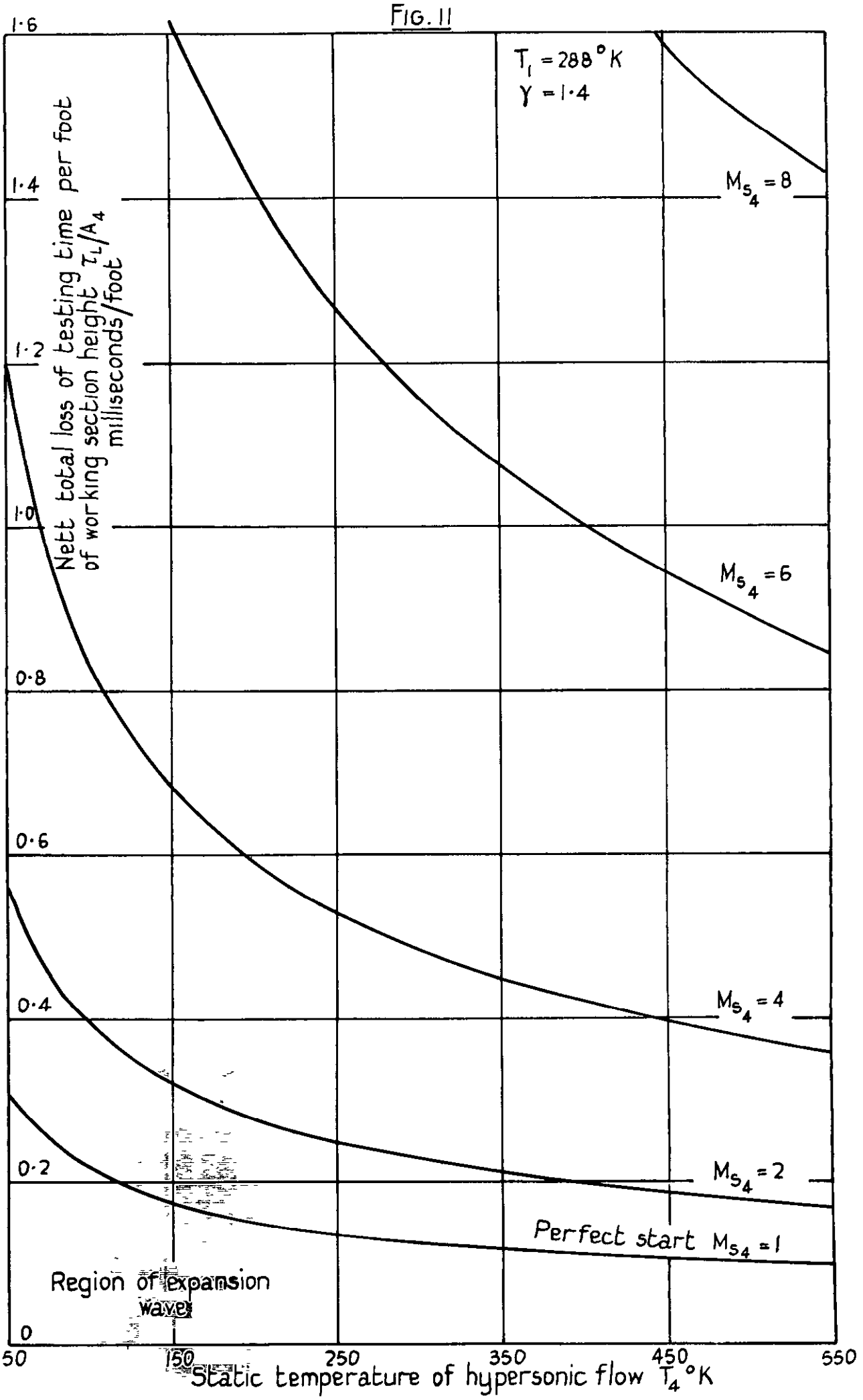

Hypersonic shock tube

Loss of testing time due to starting process. Imperfect start $M_4 = 15$

FIG 12

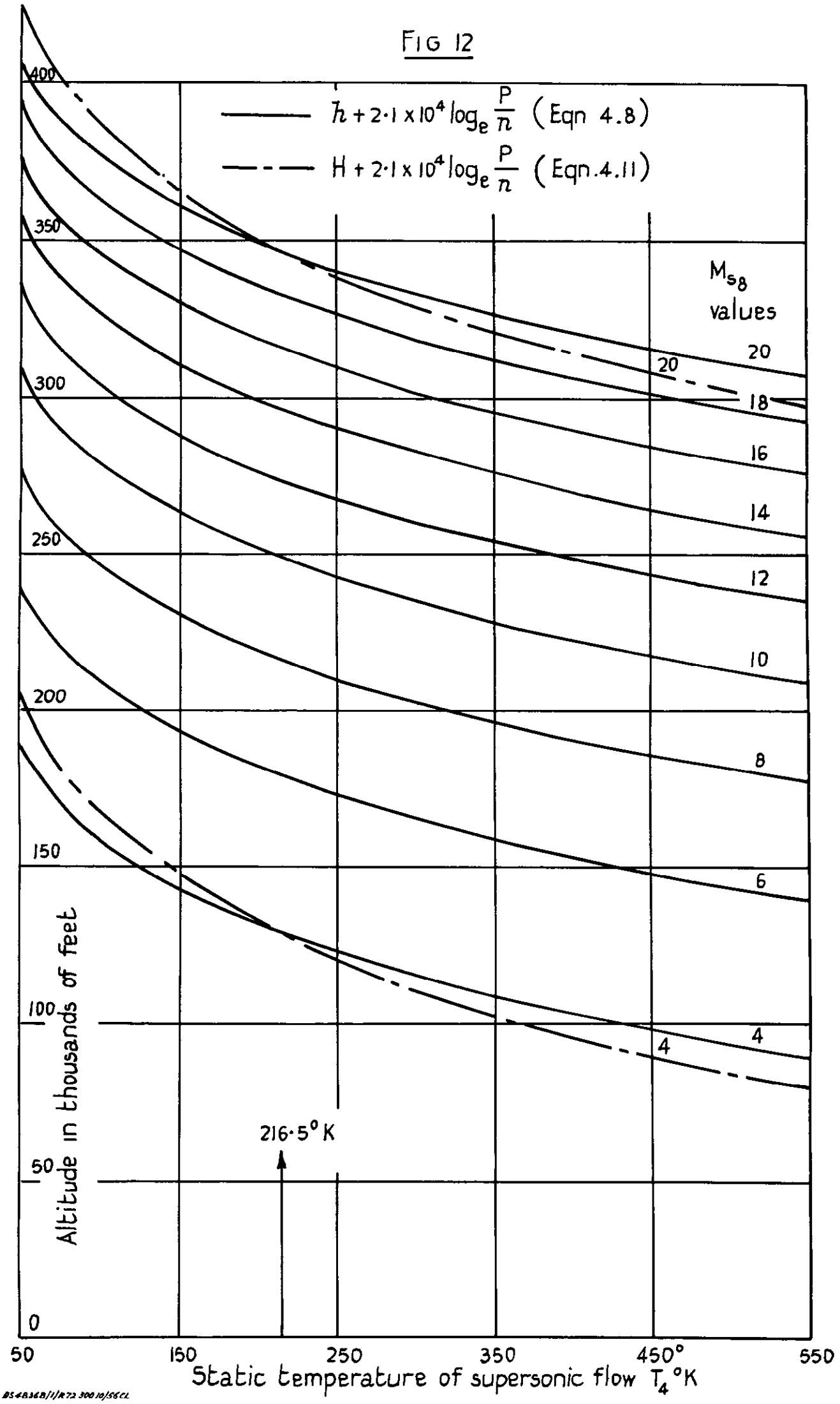

BS4836B/1/R72 300 10/56 CL

Hypersonic shock tube: Reynolds number chart.

C.P. No. 293
(18 201)
A.R C Technical Report

Printed and published by
HER MAJESTY'S STATIONERY OFFICE

To be purchased from
York House, Kingsway, London W C.2
423 Oxford Street, London W.1
P O Box 569, London S E.1
13A Castle Street, Edinburgh 2
109 St. Mary Street, Cardiff
39 King Street, Manchester 2
Tower Lane, Bristol 1
2 Edmund Street, Birmingham 3
80 Chichester Street, Belfast
or through any bookseller

Printed in Great Britain

S O Code No 23-9009-93

C.P. No. 293